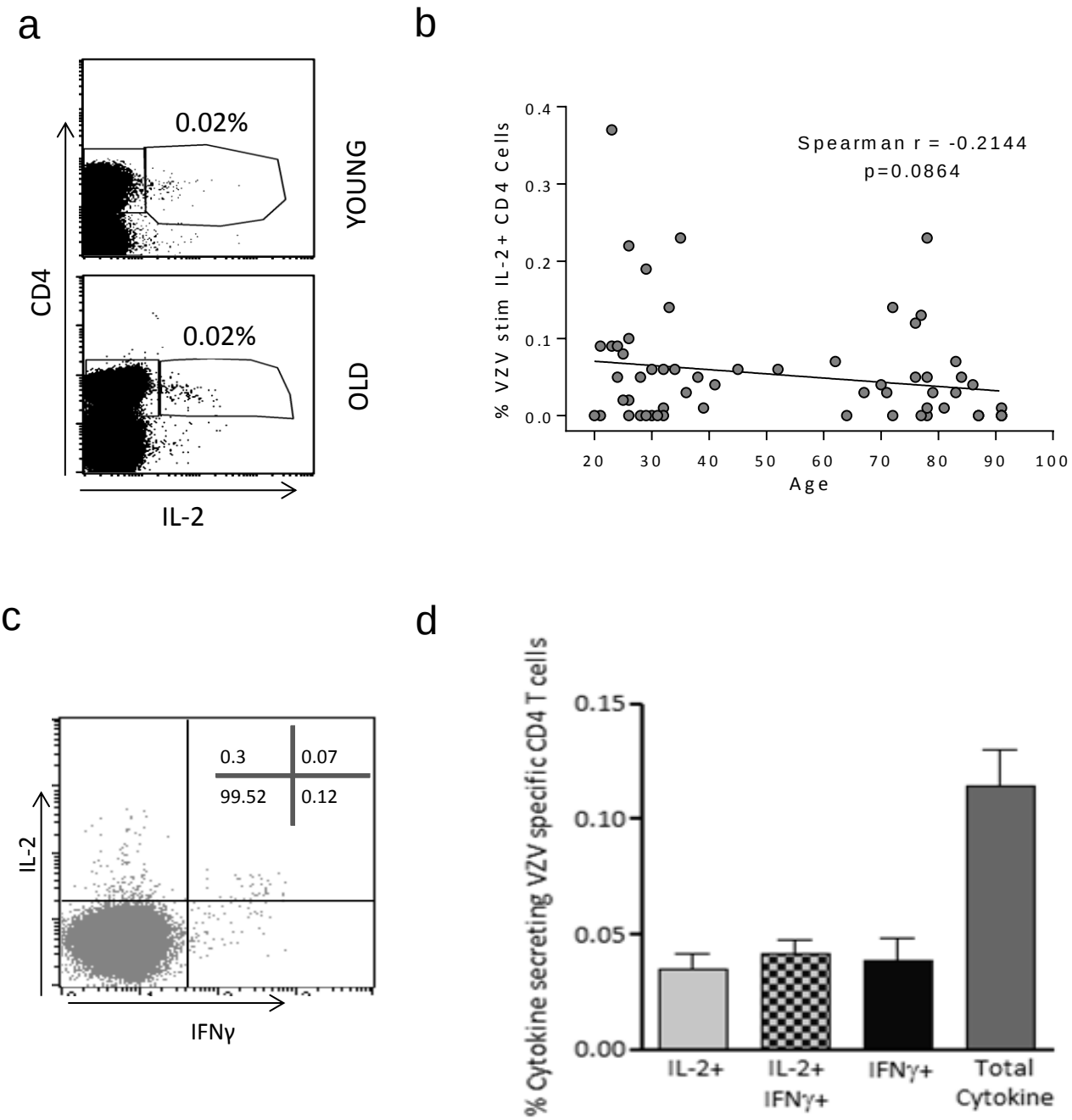

Supplementary Figure 1.The effect of age on IL-2$^+$VZV specific cells. PBMC were stimulated with VZV lysate overnight in the presence of brefeldin A, stained for IFN-γ, IL-2 and CD4 and analysed by flow cytometry. (A) Representative dot plots for IL-2 secretion in young and old. (B) Correlation with age. (C) A representative dot plot shows the distribution of IL-2 and IFN-γ secretion of gated CD4$^+$ T cells in response to VZV stimulation. (D) A bar chart summarising the percentage of CD4$^+$ T cells which secreted IL-2 alone (IL-2$^+$), IL-2 and IFN-γ (IL-2$^+$IFN-γ$^+$) or IFN-γ alone (IFN-γ$^+$) in response to VZV stimulation in 67 donors. There was no significant difference in the proportion of IL-2 or IFN-γ secreting cells using Kruskal-Wallis analysis of variance test.

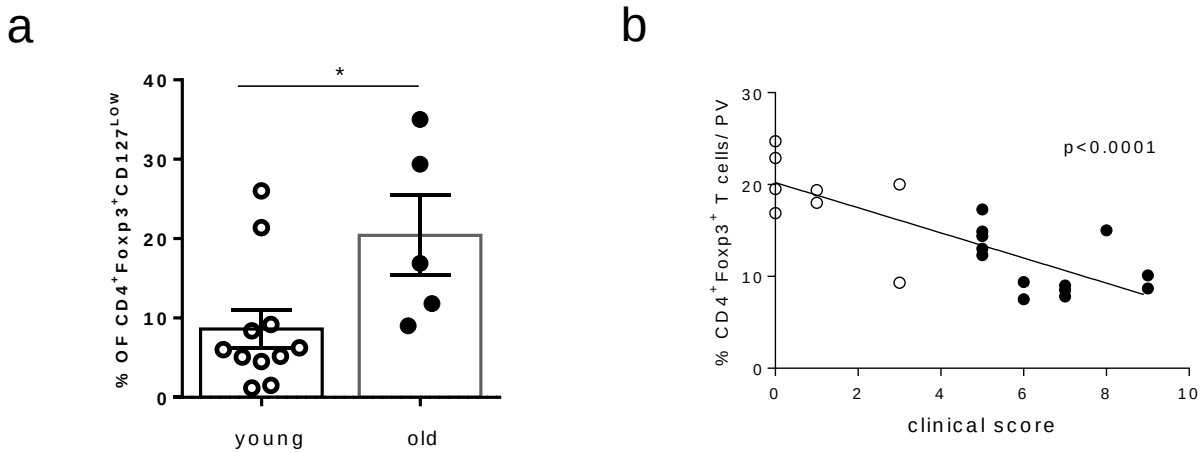

Supplementary Figure 2.The effect of age on CD4+Foxp3+ regulatory T cells in the skin. (A) PBMC and skin derived cellos were stained with CD4, Foxp3, CD127 and CD25 to enumerate the proportion of regulatory T cells in different age groups. Bars represent Mean and SEM for each age group, individual subjects are represented as separate data points. p=0.015, unpaired t-test (B) 5mm punch biopsies were collected following intradermal challenge with VZV antigen and stained for CD4 and Foxp3. Numbers of cells were counted in perivascular infiltrates (plotted as average of 5 largest perivascular infiltrates (PV) counted). Graph shows an inverse correlation between the proportion of $Foxp3^{+}$ cells within CD4 population and the clinical score (filled circles-young, open circles- old)

a

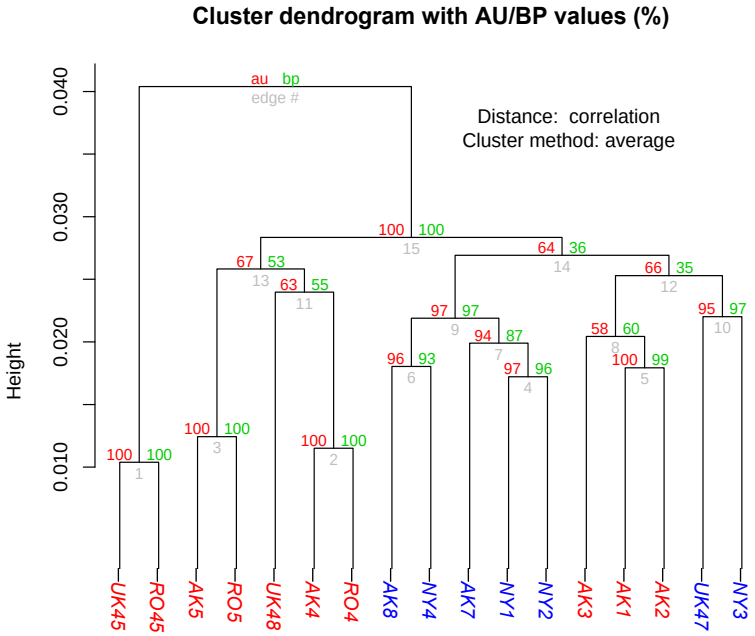

b

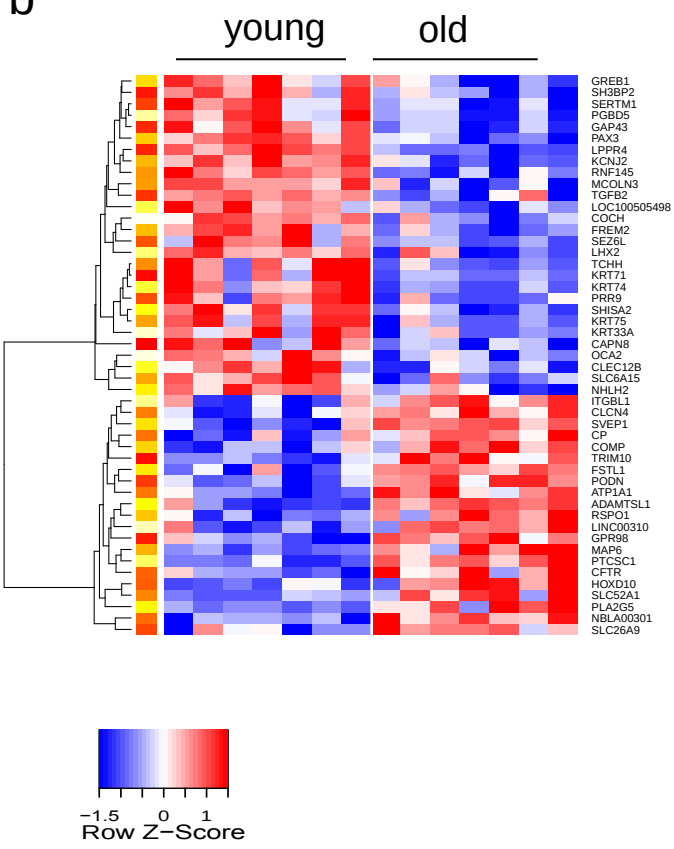

c

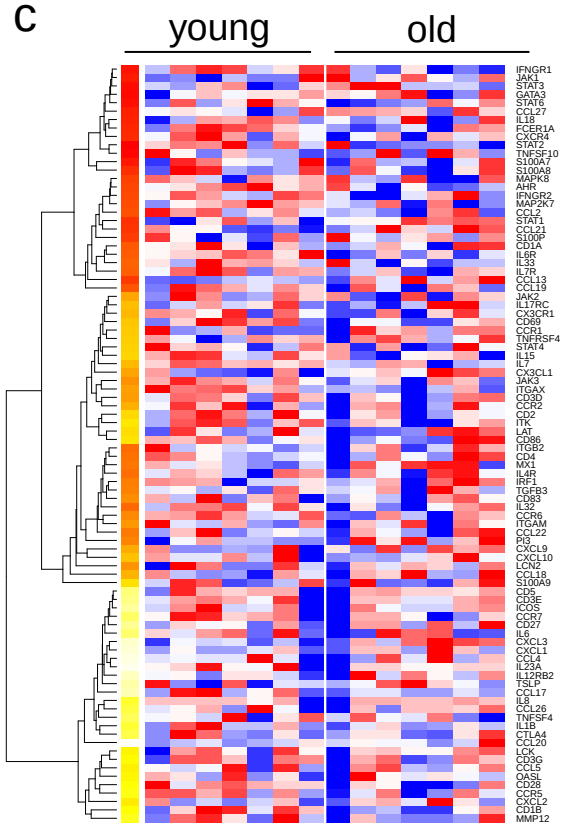

Supplementary Fig 3

d

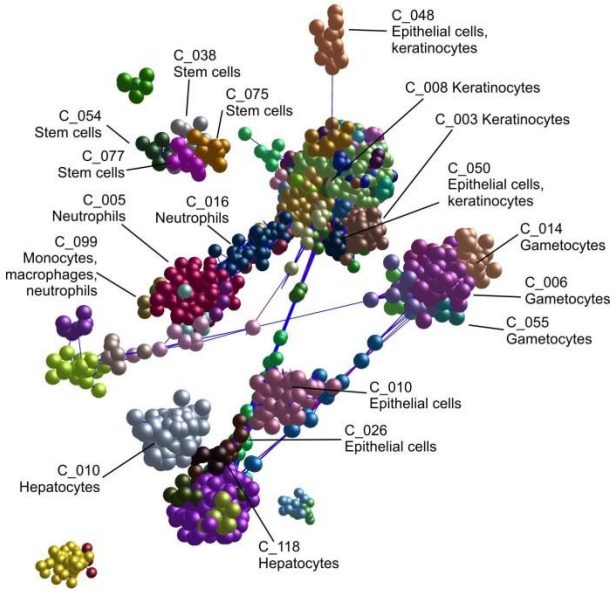

e

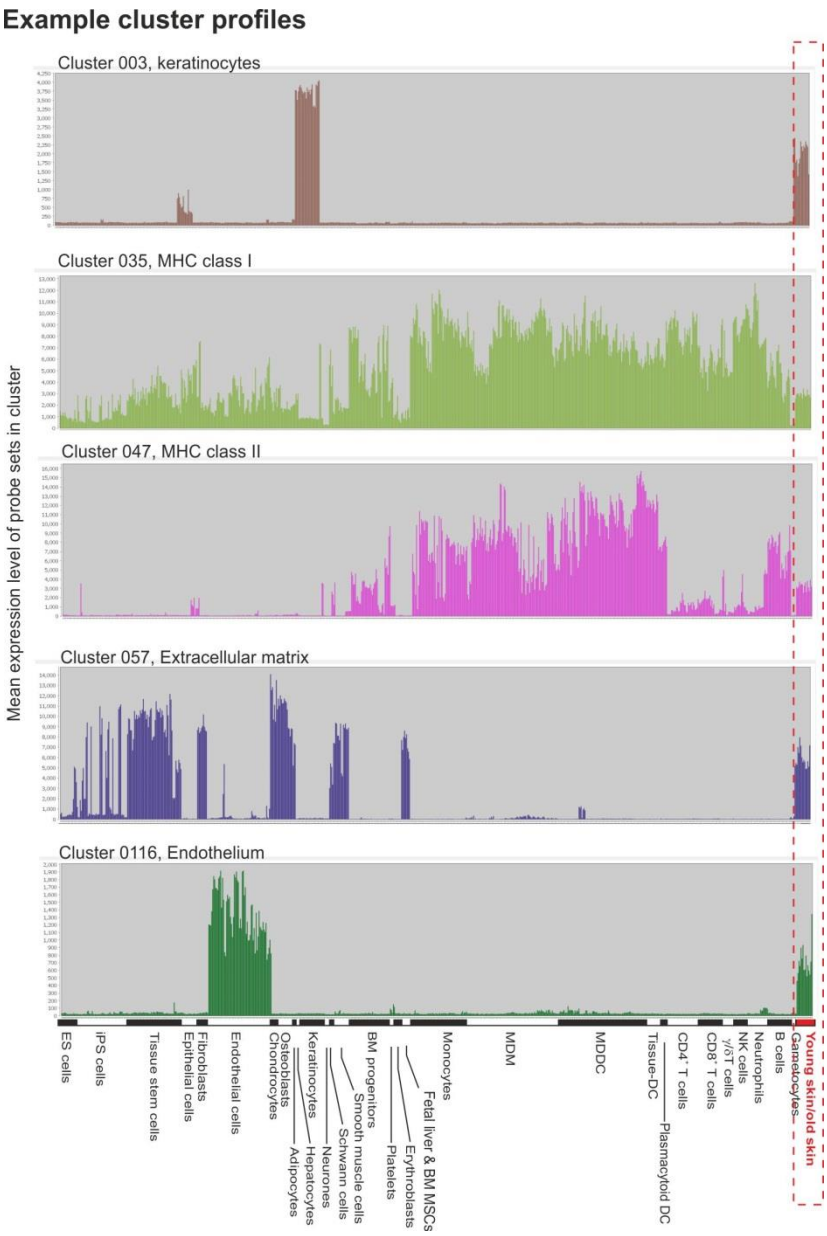

Supplementary Fig 3

Supplementary Figure 3. Transcriptomic analysis of young and old normal skin. (A) Dendogram showing the unsupervised clustering of the skin samples using the expression profiles. Simulations were run are to determine how robust the clusters to variations in the data. Clusters with high probabilities indicates stables cluster and replications from the same patient clustered together in 100% of the bootstrapping samples (eg AK5 and RO5, AK4 and RO4, UK45 and RO45). Overall no structure was identified where stable clusters were found with a pattern differentiating between young and old (indicated by blue and red color of sample ID). Similar dendograms were obtained when different agglomeration procedures where used. (B) Heatmap shows the relative expression of differentially expressed genes between young and old skin at FCH>2 and FDR>0.2. (C) Heatmap shows the relative expression of immune genes (manually curated by our lab and extensively used (38) showing no discernible pattern of expression differentiating skin from young and old healthy individuals. For each gene, only the probeset with the largest average expression is shown. (D) Network analysis of the human skin-punch biopsies and 745 primary cell gene-expression data sets using the tool BioLayout Express3D. This analysis enabled the visualization of genes within a cluster across the entire data collection. Genes with similar expression profiles are clustered together within the same region of the network graph. Nodes represent transcripts (probe sets) and the edges represent correlations between individual expression profiles above $r = 0.90$. The nodes are coloured according to the cluster to which they have been assigned. The positions of representative clusters are annotated. (E) Young and old skin samples shared similar gene cluster expression profiles. Five representative clusters derived from the network graph are shown and their mean probe set expression profiles across all data sets. The boxed area surrounded by a red line indicates the location of the young and old skin data sets. Cluster 003 contained genes that are highly expressed by keratinocytes, and cluster 116 contained endothelium-related genes. Cluster 035 contained genes encoding MHC class I, whereas cluster 047 contained genes encoding MHC class II. Cluster 057 was enriched in extracellular matrix-related genes. The genes in these clusters were expressed at similar levels across all of the young and old skin samples. ES cells, embryonic stem cells; iPS cells, induced pluoripotent stem cells; BM, bone marrow; MSC, mesenchymal stem cells; MDM, monocyte-derived macrophage; MDDC, monocyte-derived dendritic cells; NK, natural killer cells.

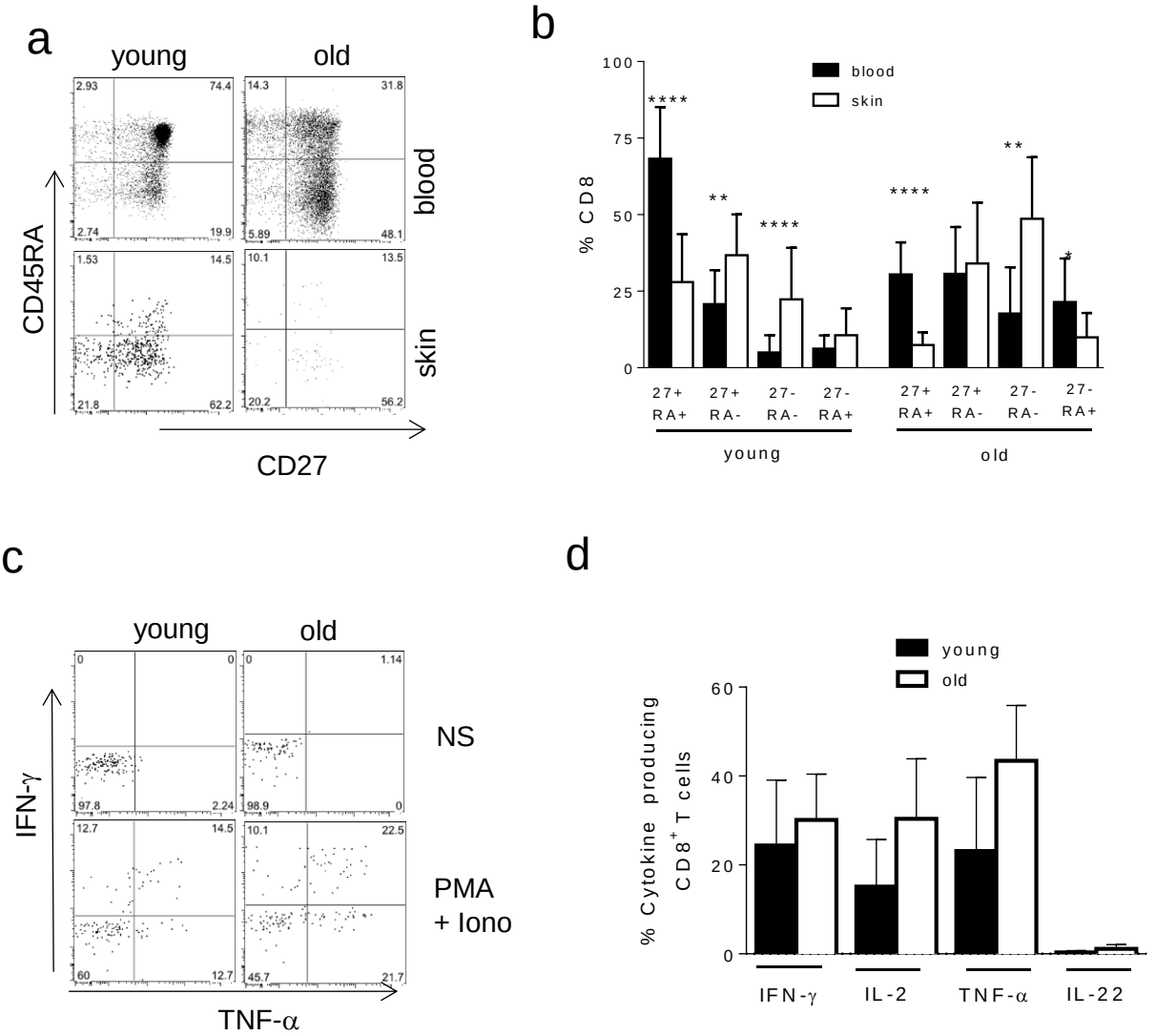

Supplementary Figure 4. Effect of age on the phenotype and function of skin resident CD8+ T cells. 5 mm punch biopsies and peripheral blood samples were collected from n=31 young and n=23 old donors. Following overnight digestion of biopsies, skin cells and PBMC were stained with CD8, CD45RA and CD27 to identify 4 differentiation subsets. Representative FACS staining of PBMC (top panels) and skin derived cells (bottom panels) from young and old donors, is shown gated on the $CD3^{+}CD8^{+}$ cells. (B) Bar chart shows cumulative data for in young and old individuals. Statistical analysis of blood and skin populations was performed using a paired t-test and p-values are indicated where relevant. (C) Skin derived leukocytes were stimulated for 5 hours with PMA and ionomycin in the presence of brefeldin A and stained for CD8, IFN-γ, IL-2, TNF-α and IL-22. Representative dot plots are shown, gated on $CD8^{+}$ cells (NS, non stimulated; PMA+Iono, PMA and ionomycin). (D) Graphs show % of $CD8^{+}$ cells staining positive for a particular cytokine (n=5-7 young and old for each cytokine).

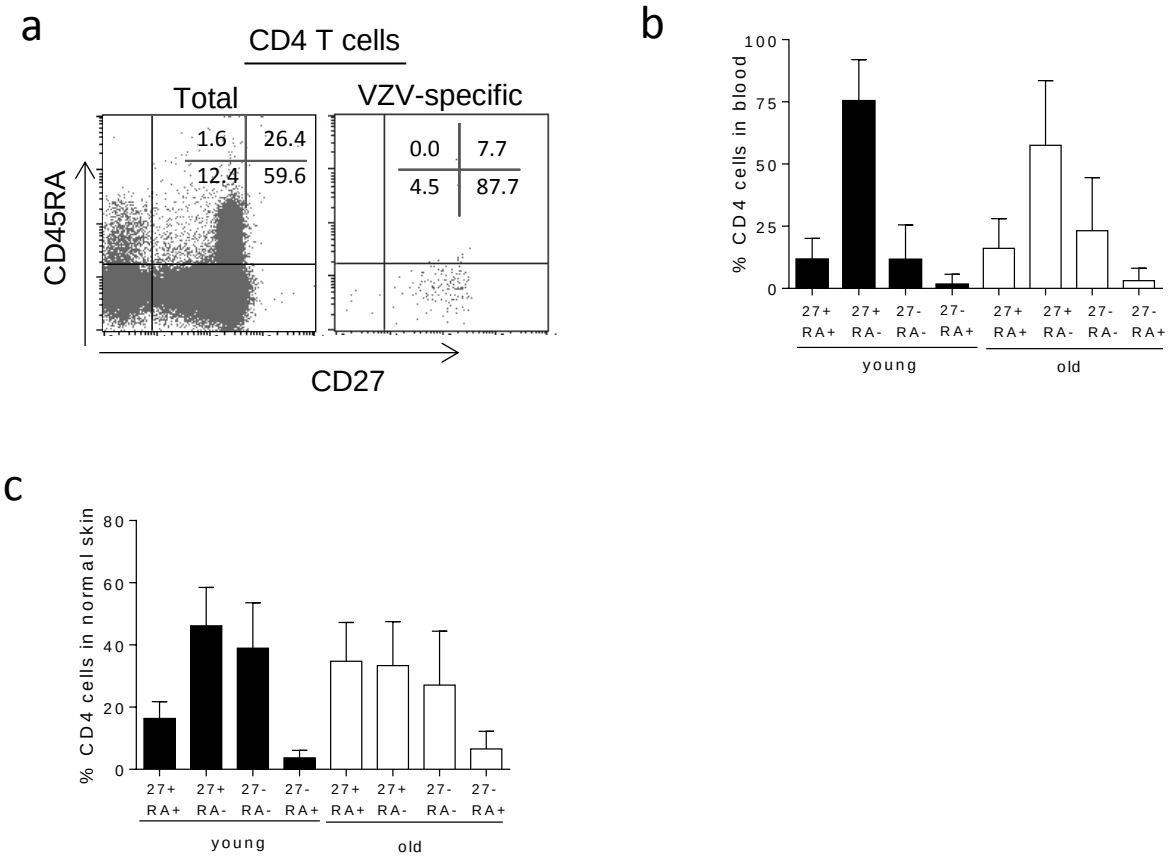

Supplementary figure 5. VZV specific cells have a central memory phenotype and there is no significant difference between young and old. PBMCs were stained with CD4, CD27, CD45RA and intracellular IFN-γ antibodies following overnight stimulation with VZV lysate in the presence of brefeldin A. Representative dot plots showing the CD27 and CD45RA phenotype of VZV specific $CD4^+$ T cells secreting IFN-γ (A) compared to the total $CD4^+$ T cell population are shown for young and old individuals. (B) Graph shows the phenotype of circulating VZV specific (IFN-γ^+) cells in young and old donors (n= 45 young, 24 old). (C) Phenotype of VZV-specific skin resident T cells. In HLA-$DR15^+$ donors skin derived cells were stained with HLA-DRB1*1501 restricted IE63 tetramer and the phenotype was compared based on CD45RA and CD27 expression.

Supplementary Table 1. List of probesets and genes within the clusters of interest derived from the network graph. Gene expression profiles in the young and aged skin samples were compared with that of a large collection of microarray data sets from distinct human primary cell populations (745 individual data sets,) using the bioinformatics tool Biolayout Express3D. 11,914 probe sets (genes) were clustered together using a Pearson correlation threshold of r=0.90 and Markov clustering algorithm of 2.2 into 140 clusters containing $\geq$ 5ptrobe sets. The contents of selected clusters of interest derived from the network graph are presented.